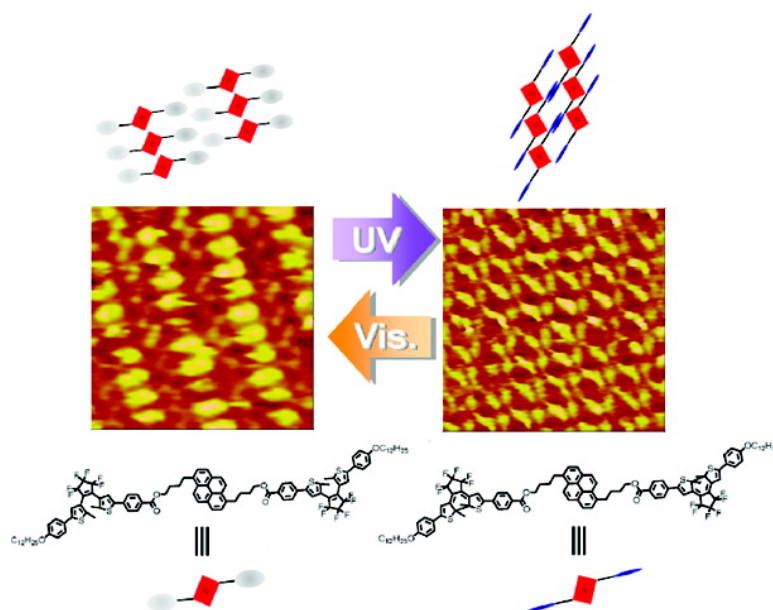


## Reversible Photoinduced Change in Molecular Ordering of Diarylethene Derivatives at a Solution/HOPG Interface

Ryota Arai, Shinobu Uemura, Masahiro Irie, and Kenji Matsuda

*J. Am. Chem. Soc.*, **2008**, 130 (29), 9371-9379 • DOI: 10.1021/ja7111041p • Publication Date (Web): 27 June 2008

Downloaded from <http://pubs.acs.org> on February 8, 2009



### More About This Article

Additional resources and features associated with this article are available within the HTML version:

- Supporting Information
- Links to the 1 articles that cite this article, as of the time of this article download
- Access to high resolution figures
- Links to articles and content related to this article
- Copyright permission to reproduce figures and/or text from this article

[View the Full Text HTML](#)

## Reversible Photoinduced Change in Molecular Ordering of Diarylethene Derivatives at a Solution–HOPG Interface

Ryota Arai,<sup>†</sup> Shinobu Uemura,<sup>‡</sup> Masahiro Irie,<sup>§</sup> and Kenji Matsuda<sup>\*,†,‡,⊥</sup>

Department of Chemistry and Biochemistry, Graduate School of Engineering, Kyushu University, 744 Motoooka, Nishi-ku, Fukuoka 819-0395, Japan, PRESTO, JST, 4-1-8 Honcho, Kawaguchi 332-0012, Japan, and Department of Chemistry, Rikkyo University, 3-34-1 Nishi-Ikebukuro, Toshima-ku, Tokyo 171-8501, Japan

Received December 12, 2007; E-mail: kmatsuda@cstf.kyushu-u.ac.jp

**Abstract:** A diarylethene–pyrene diad and a diarylethene–pyrene–diarylethene triad were synthesized to investigate the photoinduced two-dimensional ordering change at a solution–HOPG interface. The molecular arrangements were detected by STM. The different photochromic isomers showed different orderings reflecting the differences in their molecular structures. For the diarylethene–pyrene–diarylethene triad, a new ordering appeared upon irradiation with UV light and returned to the original ordering upon subsequent irradiation with visible light. The new arrangement was assigned to the ordering of the closed–closed isomers based on the images of the isolated open- and closed-isomers. The relationship between the nature of the two-dimensional ordering and the molecular structure is discussed.

### Introduction

The two-dimensional (2D) self-assembly of organic compounds on a solid surface has become a topic of considerable interest in materials science, organic electronics, and molecular-scale electronics.<sup>1</sup> In particular, photo- and electrochromic compounds are attracting attention from the viewpoint of their application as molecular switches.<sup>2</sup> Although such molecular switches are expected to regulate the flow of the electrical signals through the molecule, to assemble the molecules in the desired structure is indispensable for the successful operation of these molecular devices.

Scanning tunneling microscopy (STM) is a powerful tool for investigating the 2D self-assembled structures with atomic resolution even at room temperature.<sup>3</sup> Using this technique, it is possible to determine the molecular orientation and packing in the 2D crystalline state on surfaces and at interfaces.<sup>4</sup>

At liquid–solid interfaces, self-assembled structures are readily formed due to the coexistence of adsorption and desorption processes.<sup>5</sup> Hydrogen bonding,<sup>6</sup> metal–ligand complexation,<sup>7</sup> and charge-transfer interaction<sup>8</sup> regulate the direction of the 2D ordering and increase the stability of the ordering.

Several attempts to control the ordering by external stimuli have recently been reported. The ordering change has been induced by heat,<sup>9</sup> light,<sup>10</sup> and the addition of appropriate molecules.<sup>11</sup>

In this paper, we report on the reversible photoinduced 2D molecular ordering change of photochromic diarylethenes at the

<sup>†</sup> Kyushu University.

<sup>‡</sup> PRESTO, JST.

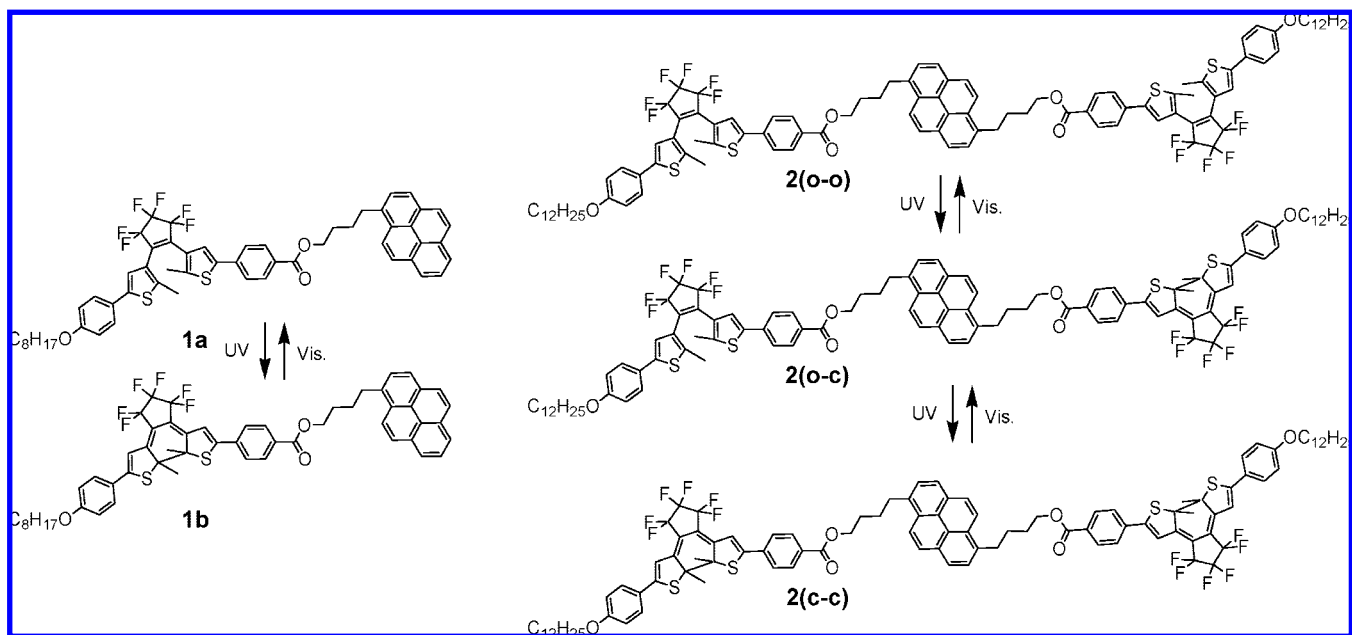
<sup>§</sup> Rikkyo University.

<sup>⊥</sup> Present address: Department of Synthetic Chemistry and Biological Chemistry, Graduate School of Engineering, Kyoto University, Katsura, Nishikyo-ku, Kyoto 615-8510, Japan.

- (1) (a) Gimzewski, J. K.; Joachim, C. *Science* **1999**, *283*, 1683. (b) De Feyter, S.; De Schryver, F. C. *Chem. Soc. Rev.* **2003**, *32*, 139–150.
- (2) Feringa, B. L., Ed. *Molecular Switches*; Wiley-VCH: Weinheim, Germany, 2001.
- (3) (a) Kim, Y.; Komeda, T.; Kawai, M. *Phys. Rev. Lett.* **2002**, *89*, 126104. (b) Henzl, J.; Mehlhorn, M.; Gawronski, H.; Rieder, K.-H.; Morgenstern, K. *Angew. Chem., Int. Ed.* **2006**, *45*, 603606. (c) Comstock, M. J.; Levy, N.; Kirakosian, A.; Cho, J.; Lauterwasser, F.; Harvey, J. H.; Strubbe, D. A.; Fréchet, J. M. J.; Trauner, D.; Louie, S. G.; Crommie, M. F. *Phys. Rev. Lett.* **2007**, *99*, 038301.

- (4) (a) Böhringer, M.; Morgenstern, K.; Schneider, W.-D.; Berndt, R. *Angew. Chem., Int. Ed.* **1999**, *38*, 821–823. (b) Florio, G. M.; Klare, J. E.; Pasamba, M. O.; Werblowsky, T. L.; Hyers, M.; Berne, B. J.; Hybertsen, M. S.; Nuckolls, C.; Flynn, G. W. *Langmuir* **2006**, *22*, 10003–10006. (c) Furukawa, S.; Uji-i, H.; Tahara, K.; Ichikawa, T.; Sonoda, M.; De Schryver, F. C.; Tobe, Y.; De Feyter, S. *J. Am. Chem. Soc.* **2006**, *128*, 3502–3503.
- (5) (a) Rabe, J. P.; Buchholz, S. *Science* **1991**, *253*, 424–427. (b) De Feyter, S.; Gesquiere, A.; Abdel-Mottaleb, M. M.; Grim, P. C. M.; De Schryver, F. C.; Meiners, C.; Sieffert, M.; Valiyaveetil, S.; Müllen, K. *Acc. Chem. Res.* **2000**, *33*, 520–531. (c) Cyr, B.; Venkataraman, D. M.; Flynn, G. W. *Chem. Mater.* **1996**, *8*, 1600–1615. (d) Mamdouh, W.; Uji-i, H.; Ladislav, J. S.; Dulcey, A. E.; Percec, V.; De Schryver, F. C.; De Feyter, S. *J. Am. Chem. Soc.* **2006**, *128*, 317–325.
- (6) (a) Eichhorst-Gerner, K.; Stable, A.; Moessner, G.; Declercq, D.; Valiyaveetil, S.; Enkelmann, V.; Müllen, K.; Rabe, J. P. *Angew. Chem., Int. Ed.* **1996**, *35*, 1492–1495. (b) Puigmarti-Luis, J.; Minoia, A.; Uji-i, H.; Rovira, C.; Cornil, J.; De Feyter, S.; Lazzaroni, R.; Amabilino, D. B. *J. Am. Chem. Soc.* **2006**, *128*, 12602–12603.
- (7) Zell, P.; Mögele, F.; Ziener, U.; Rieger, B. *Chem. Eur. J.* **2006**, *12*, 3847–3857.
- (8) Samori, P.; Yin, X.; Tchegbotareva, N.; Wang, Z.; Pakula, T.; Jäckel, Watson, M. D.; Venturini, A.; Müllen, K.; Rabe, J. P. *J. Am. Chem. Soc.* **2004**, *126*, 35673575.
- (9) Rohde, D.; Yan, C.-J.; Wan, L.-J. *Angew. Chem., Int. Ed.* **2006**, *45*, 3996–4000.
- (10) (a) Heinz, R.; Stabel, A.; Rabe, J. P.; Wegner, G.; De Schryver, F. C.; Corens, D.; Dehaen, W.; Stüling, C. *Angew. Chem., Int. Ed.* **1994**, *33*, 2080–2083. (b) Vanoppen, P.; Grim, P. C. M.; Rücker, M.; De Feyter, S.; Moessner, G.; Valiyaveetil, S.; Müllen, K.; De Schryver, F. C. *J. Phys. Chem.* **1996**, *100*, 19636–19641. (c) Miura, A.; De Feyter, S.; Abdel-Mottaleb, M. M. S.; Gesquiere, A.; Grim, P. C. M.; Moessner, G.; Sieffert, M.; Klapper, M.; Müllen, K.; De Schryver, F. C. *Langmuir* **2003**, *19*, 6474–6482. (d) Xu, L.-P.; Wan, L.-J. *J. Phys. Chem. B* **2006**, *110*, 3185–3188.
- (11) Furukawa, S.; Tahara, K.; De Schryver, F. C.; Van der Auweraer, M.; Tobe, Y.; De Feyter, S. *Angew. Chem., Int. Ed.* **2007**, *46*, 2831–2834.

Scheme 1. Photochromic Reaction of Compounds 1 and 2



interface between a solution and highly oriented pyrolytic graphite (HOPG). Diarylethene derivatives are well-known fatigue-resistant photochromic compounds,<sup>12</sup> which undergo cyclization/cycloreversion reactions between the open- and closed-ring isomers. The photochemical reaction brings about the switching of the  $\pi$ -conjugation and molecular planarity.<sup>13</sup> Since both isomers are thermally stable, it is not necessary to take into account a thermal reaction.<sup>14</sup> The relationship between the molecular structure and the 2D assembled structure is discussed.

## Results and Discussion

**Molecular Design and Syntheses of Compounds 1 and 2.** The diarylethene–pyrene diad **1** and diarylethene–pyrene–diarylethene triad **2** were designed and synthesized according to Schemes 1–3. The long alkyl chain and pyrene were introduced into the diarylethene in order to stabilize the 2D structure. Pyrene interacts with HOPG due to extended planar  $\pi$ -conjugation.<sup>15</sup> The alkyl chains are also effective at interacting with the HOPG substrate. The presence of the short alkyl chain between the diarylethene and pyrene increases the flexibility. For the aromatic photochromic core, 1,2-bis(2-methyl-5-phenyl-3-thienyl)perfluorocyclopentene was chosen.

The syntheses of compounds **1** and **2** were carried out as described in Schemes 2 and 3, respectively. A diarylethene with a formyl group was synthesized using an ethylene glycol protecting group. After oxidation to a carboxylic acid, DCC coupling with an alcohol-carrying pyrene gave the final product. The structures were confirmed by <sup>1</sup>H NMR and high-resolution mass spectroscopies.

**UV–Vis Absorption Spectra of 1 and 2.** Compounds **1** and **2** underwent photochromic reactions upon irradiation with UV and visible light in solution (Figure 1). Upon irradiation with

UV light ( $\lambda = 313$  nm), the colorless solution turned blue, and the solution returned to colorless by irradiation with visible light ( $\lambda > 480$  nm). A comparison of the absorption spectra with the pure closed-ring isomer separated by HPLC showed that the conversion from the open- to the closed-ring isomer under irradiation with 313 nm light was 97% for diarylethene **1**. For the diarylethene dimer **2**, the ratio of the open–open, the open–closed, and the closed–closed isomers in the photostationary state under irradiation with 313 nm light was 0.1:8.2:91.7, respectively, which was determined by HPLC analysis.

**2(o–o)** has two diarylethene moieties. Upon irradiation with UV light, both diarylethene units underwent efficient cyclization reactions, and a very high conversion up to 92% was attained. This result indicates that the two chromophores undergo cyclization independently and the interaction between the two closed-ring isomers is very small due to the broken  $\pi$ -conjugation and the large distance between the diarylethenes.

**X-ray Crystallographic Analysis of 1a.** The X-ray diffraction experiment was performed on a single crystal of the open-ring isomer **1a**. The ORTEP drawing is shown in Figure 2a.<sup>16</sup> The crystallographic structure shows that the thiophene, benzene, and pyrene rings exist almost in the same plane. However, the octyloxy chain is not coplanar with the pyrene ring. In the crystal, the pyrene rings form a 2D arrangement, since the pyrene rings are packed in the same direction. The distance between the pyrene layers is 0.75 nm, so that  $\pi$ – $\pi$  stacking between the pyrenes is not effective. Figure 2b shows the 2D arrangement viewed normal to the pyrene plane. The unit cell parameters of this 2D arrangement are as follows:  $a = 1.29$  nm;  $b = 2.58$  nm;  $\alpha = 96.5^\circ$ .

**STM Measurements of 1.** STM images of the open-ring isomer **1a** were obtained at the 1-phenyloctane–HOPG interface. As shown in Figure 3a, compound **1a** formed a well-

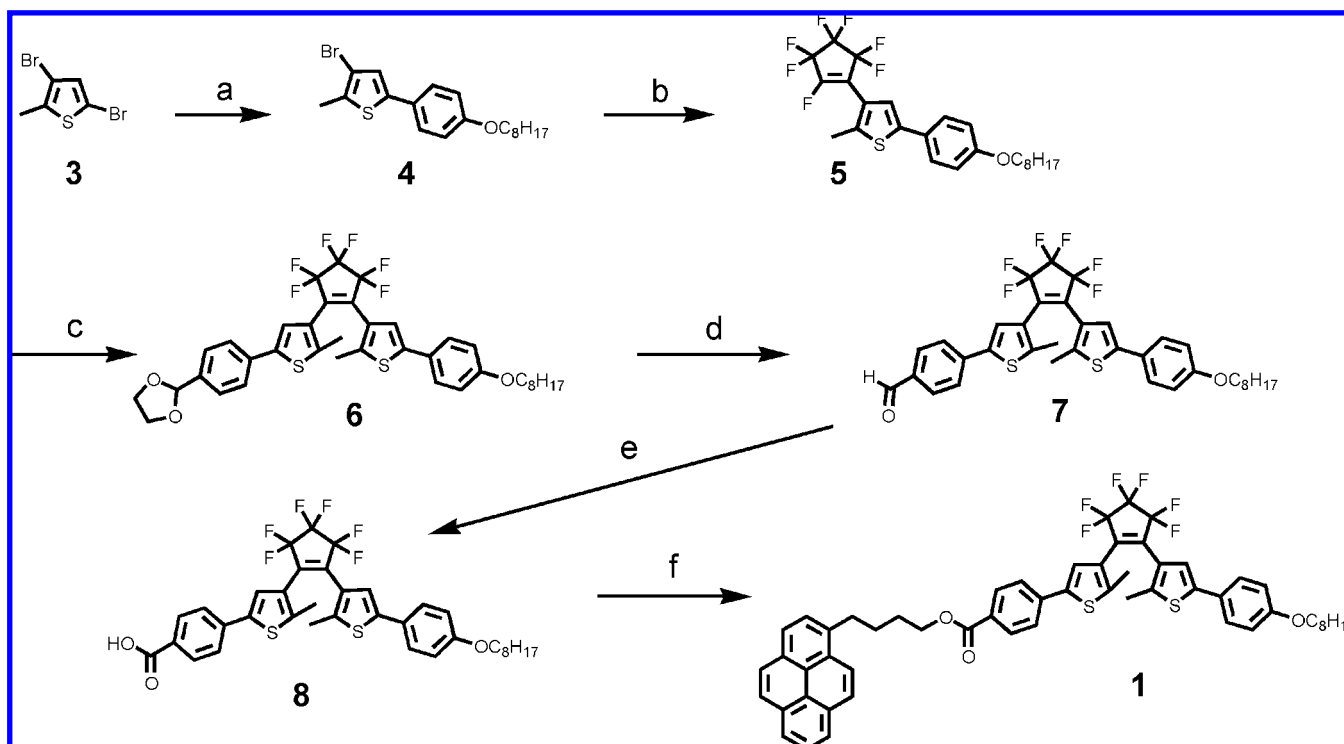
(12) Irie, M. *Chem. Rev.* **2000**, *100*, 1685–1716. Matsuda, K.; Irie, M. *J. Photochem. Photobiol. C* **2004**, *5*, 169–182.

(13) Irie, M.; Kobatake, S.; Horichi, M. *Science* **2001**, *291*, 1769–1772.

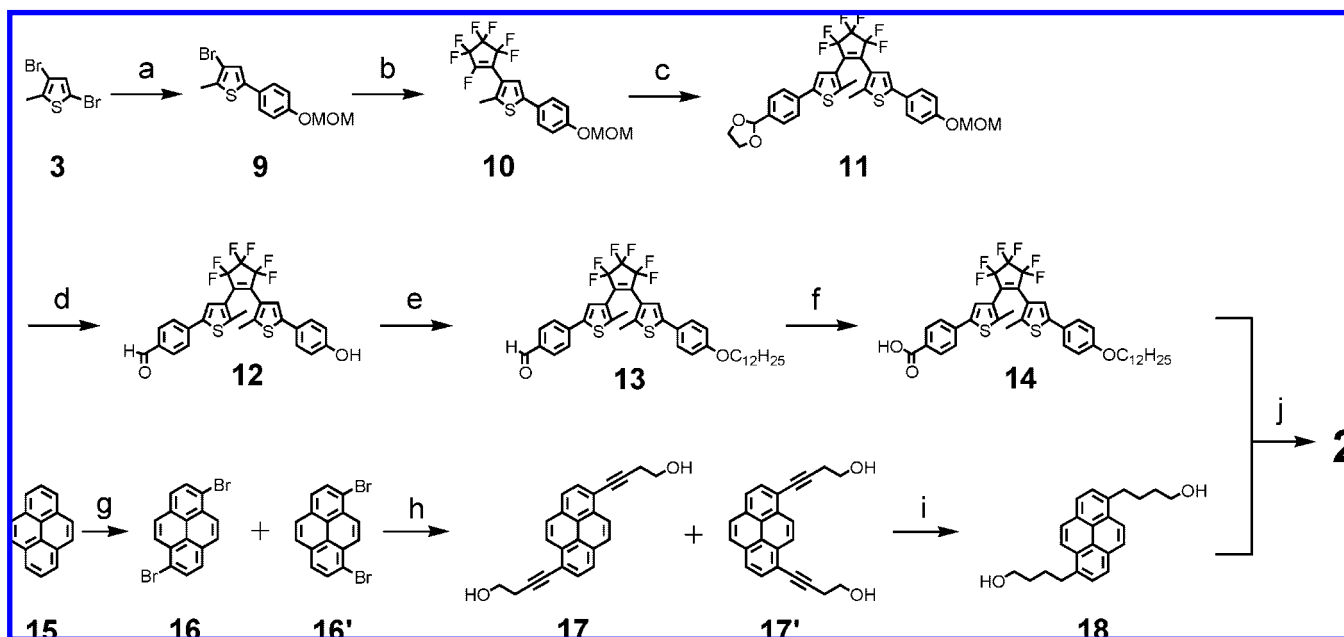
(14) Nakamura, S.; Irie, M. *J. Org. Chem.* **1988**, *53*, 6136–6138.

(15) Uji-i, H.; Yoshidome, M.; Hobley, J.; Hatanaka, K.; Fukumura, H. *Phys. Chem. Chem. Phys.* **2003**, *5*, 4231–4235.

(16) Crystal data for **1a**: C<sub>56</sub>H<sub>50</sub>F<sub>6</sub>O<sub>3</sub>S<sub>2</sub>, FW = 949.12, triclinic,  $P\bar{1}$ ,  $a = 8.324(3)$  Å,  $b = 12.866(4)$  Å,  $c = 23.101(8)$  Å,  $\alpha = 83.494(5)^\circ$ ,  $\beta = 80.571(5)^\circ$ ,  $\gamma = 82.972(5)^\circ$ ,  $V = 2411.1(14)$  Å<sup>3</sup>,  $Z = 2$ , Data/restraints/parameters = 3024/0/607, R1 [ $I > 2\sigma(I)$ ] = 0.0611, wR2 (all data) = 0.1799. CCDC 650023 contains the supplementary crystallographic data.

Scheme 2. Synthesis of Compound 1<sup>a</sup>

<sup>a</sup> Reagents and conditions: (a) *n*-BuLi, dry THF, (BuO)<sub>3</sub>B, and then 4-iodooctyloxybenzene, Na<sub>2</sub>CO<sub>3</sub>aq, Pd(PPh<sub>3</sub>)<sub>4</sub>, 54%; (b) *n*-BuLi, perfluorocyclopentene, dry THF, 88%; (c) *n*-BuLi, 3-bromo-5-(4-(2,5-dioxolanyl)phenyl)-2-methylthiophene, dry THF, 60%; (d) pyridinium *p*-toluenesulfonate, acetone, 77%; (e) Jones reagent, acetone, 77%; (f) 1-pyrenylbutanol, DCC, DMAP, DMF, 24%.

Scheme 3. Synthesis of Compound 2<sup>a</sup>

<sup>a</sup> Reagents and conditions: (a) *n*-BuLi, dry THF, (BuO)<sub>3</sub>B, and then 1-bromo-4-methoxymethoxy-benzene, Na<sub>2</sub>CO<sub>3</sub> aq, Pd(PPh<sub>3</sub>)<sub>4</sub>, 79%; (b) *n*-BuLi, perfluorocyclopentene, dry THF, 77%; (c) *n*-BuLi, 3-bromo-5-(4-(2,5-dioxolanyl)phenyl)-2-methylthiophene, dry THF, 89%; (d) HCl aq (35%), THF, quant; (e) 1-bromododecane, KOH, KI, ethanol, 96%; (f) Jones reagent, acetone, 77%; (g) BTMA Br<sub>3</sub>, ZnCl<sub>2</sub>, MeOH/CH<sub>2</sub>Cl<sub>2</sub> (2/5), quant; (h) 3-butyne-1-ol, CuI, PdCl<sub>2</sub>(PPh<sub>3</sub>)<sub>2</sub>, morpholine, 32%; (i) H<sub>2</sub>, 5% Pd/C, AcOEt, quant.; (j) DCC, DMAP, CH<sub>2</sub>Cl<sub>2</sub>, 45%.

ordered 2D molecular arrangement over a wide domain (larger than the scanning area of 100 × 100 nm<sup>2</sup>). According to the previous report on the 2D structure of a pyrene-containing molecule,<sup>15</sup> the bright elliptic spots in Figure 3b are assigned to the pyrene moiety of compound 1a, and the small bright spots are

assigned to the diarylethene moiety. The octyloxy chains could not be observed at any bias voltage or set point current. The unit cell parameters of the 2D structure are  $a = 1.4 \pm 0.1$  nm,  $b = 2.6 \pm 0.1$  nm, and  $\alpha = 115 \pm 2^\circ$ . Since no stable 2D molecular structure was observed for those molecules synthesized without

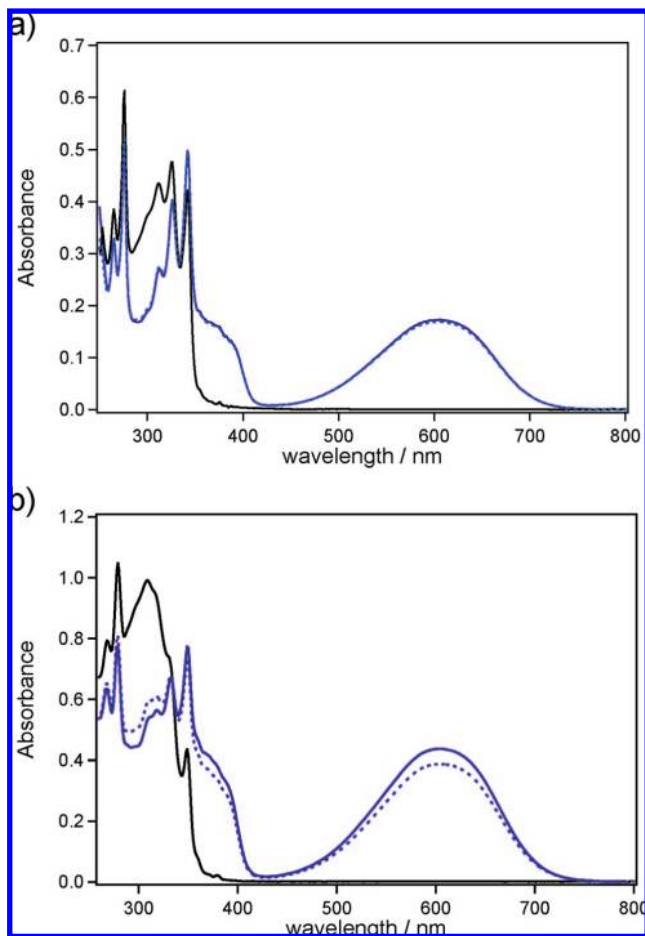


**Figure 1.** (a) Photochromic absorption spectral change of compound **1** in ethyl acetate ( $8.6 \times 10^{-6}$  M). Black line: open-ring isomer; blue solid line: closed-ring isomer; blue dotted line: in the photostationary state under irradiation with 313 nm light. Conversion = 97%. (b) Photochromic spectral change of compound **2** in ethyl acetate ( $1.0 \times 10^{-5}$  M). Black line: open–open isomer; blue solid line: closed–closed isomer; blue dotted line: in the photostationary state under irradiation with 313 nm light. In the photostationary state,  $2(\text{o}-\text{o}):2(\text{o}-\text{c}):2(\text{c}-\text{c}) = 0.1:8.2:91.7$ .

an octyloxy chain, the octyloxy chain is effectively physisorbed on HOPG and indispensable to stabilize the 2D ordering.

This structure was explained on the basis of the molecular model constructed by molecular mechanics calculations (MacroModel, OPLS\_2005) (Figure 3c).<sup>17</sup> In contrast to the bent structure observed in the bulk crystal, the molecule was calculated to have a planar structure in gas phase. The total energy of the twisted isomer, in which the pyrene ring and the diarylethene are perpendicular each other, was found to be located ca. 0.5 kJ/mol higher in energy than the planar isomer, in which the pyrene ring and the diarylethene are parallel. The calculation result indicates that the difference in the total energy between the rotational isomers is very small. The small energy difference suggests that the molecular conformation can be easily affected by intermolecular interaction between adjacent molecules or the interaction between the molecule and the HOPG surface.

By comparing the molecular packing in the bulk crystal with the molecular arrangement on the HOPG substrate, both sets

(17) The molecular modeling using MacroModel has been carried out for all the molecules studied by STM. The results of the calculation and the optimized Cartesian coordinates are shown in Supporting Information.

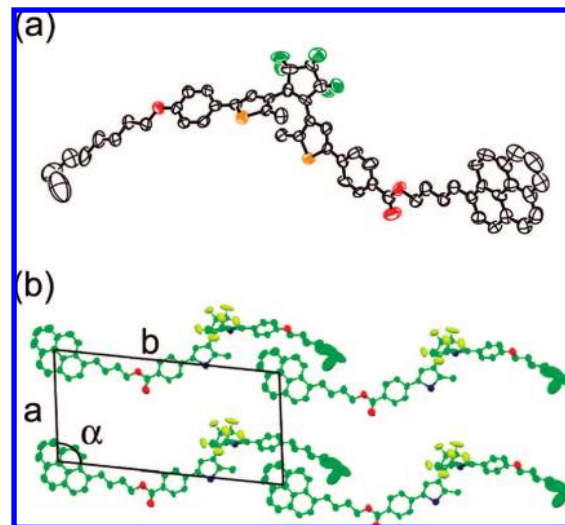


**Figure 2.** (a) ORTEP drawing of the X-ray crystallographic structure of compound **1a**. Hydrogen atoms are omitted for clarity. (b) 2D arrangement of the molecules viewed normal to the pyrene plane.

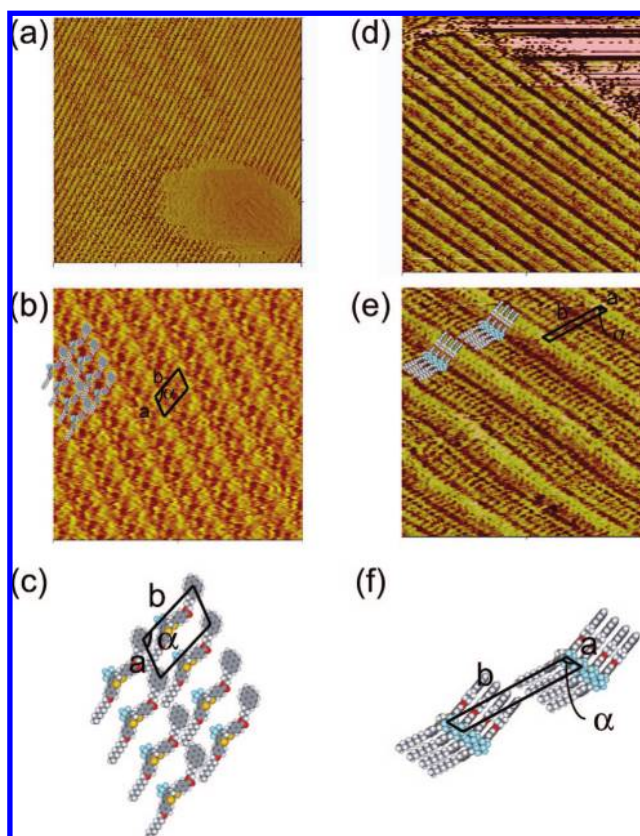


**Figure 3.** STM images of **1** at the interface of 1-phenyloctane–HOPG: (a) Open-ring isomer **1a** ( $50 \times 50$  nm<sup>2</sup>,  $I_{\text{set}} = 10$  pA,  $V_{\text{bias}} = -1.5$  V). (b) Small-area image of **1a** ( $20 \times 20$  nm<sup>2</sup>,  $I_{\text{set}} = 30$  pA,  $V_{\text{bias}} = -1.35$  V). (c) Structural model of arrangement of **1a**. (d) Closed-ring isomer **1b** ( $50 \times 50$  nm<sup>2</sup>,  $I_{\text{set}} = 20$  pA,  $V_{\text{bias}} = -1.4$  V). (e) Small-area image of **1b** ( $20 \times 20$  nm<sup>2</sup>,  $I_{\text{set}} = 40$  pA,  $V_{\text{bias}} = -1.3$  V). (f) Structural model of arrangement of **1b**.

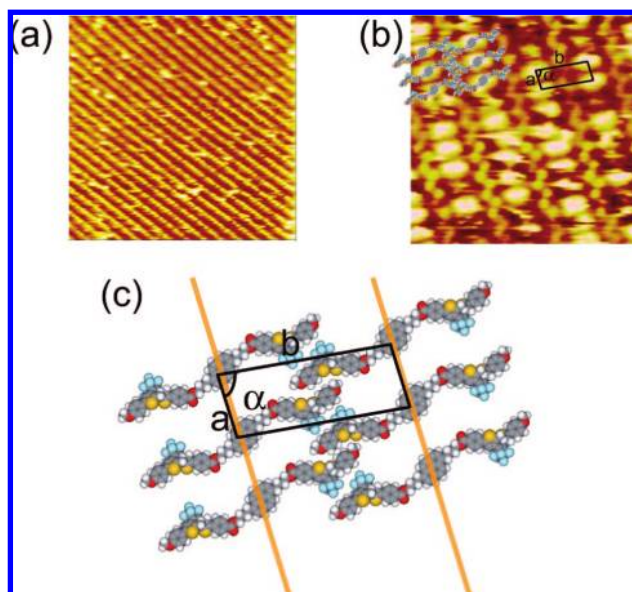
of unit cell parameters are found to be similar, but the length of the 2D unit cell observed by STM is slightly longer than that observed in the bulk crystal. This suggests that the molecular packing on the HOPG surface is looser than that in the single crystal. Because of the physisorption of both the octyloxy chain and pyrene,  $b$  in Figure 3c is longer than  $b$  in Figure 2b.

Figure 3d displays STM images of the closed-ring isomer **1b**. The unit cell parameters of the 2D structure are  $a = 0.5 \pm 0.04$  nm,  $b = 4.9 \pm 0.1$  nm, and  $\alpha = 109 \pm 6^\circ$ . This ordering was not always observed. In fact, most of the time, no ordering was observed. This result indicates that this ordering is less stable than that of **1a**. As shown in the small-area image, the 2D structure of compound **1b** differs from that of compound **1a** (Figure 3e). The molecules pack more densely than those in the structure of **1a**. The image of **1b** is explained by the calculated model shown in Figure 3f. Unlike the open-ring isomer **1a**, in which the pyrene ring is lying parallel to the HOPG surface, the pyrene ring of **1b** is lying perpendicular to the HOPG surface. Compound **1b** is thought to have less interaction with HOPG in comparison with **1a**, and the 2D structure of **1b** is therefore less stable than the 2D structure of **1a**. The diarylethene open-ring isomer has a twisted structure but the closed-ring isomer has a flat thin structure. This difference provides a significant effect on the stacking of the molecule, an effect which has been suggested by studies of the solution and crystal.<sup>18</sup>

When the arrangement of the open-ring isomer **1a** was irradiated sufficiently with UV light *in situ*, the image disappeared. Because the adlayer is a monomolecular layer, most of the molecules exist in the solution rather than at the interface. Therefore, most of the photochromic reactions take place in the solution not at the interface. When the contents of the solution phase are thereby changed, adsorption and desorption processes exchange molecules between the interface and the solution.<sup>1</sup> The photogenerated closed-ring isomer **1b** probably disturbs the adsorption of the open-ring isomer **1a**. We also tried to measure the STM image of a 6:4 mixture of **1a** and **1b**, but no ordering was observed. This result indicates that the existence of **1b** disturbs the adsorption of **1a**.

**STM Measurements of 2.** Figure 4 shows STM images of the open–open isomer of the diarylethene dimer **2(o–o)** at the octanoic acid–HOPG interface. As shown in Figure 4a, **2(o–o)** formed a well-ordered 2D molecular assembly, and the domain was larger than the scanning area of 100 nm<sup>2</sup>. The arrangement consists of parallel lines with spacing of 5.8 nm. Each line has a lamellar structure of bright lines consisting of three bright spots (Figure 4b). Considering that the pyrene moiety gives a bright spot,<sup>15</sup> the brightest spot in the middle is assigned as the pyrene moiety, and the other bright spots are assigned as diarylethene moieties in a similar manner as in the case of compound **1**. The unit cell parameters are  $a = 2.4 \pm 0.2$  nm,  $b = 6.3 \pm 0.2$  nm, and  $\alpha = 87 \pm 2^\circ$ . The molecular packing was explained using a molecular model constructed from the result of molecular mechanics calculation of molecules without alkyl chains (Figure 4c).<sup>17</sup> In the STM images, the alkyl chain sandwiched between the aromatic moieties is not observed. The calculation result shows that the total energy of the planar isomer, in which the pyrene ring and two diarylethenes are parallel, was the lowest, but the energy difference between the isomers is less than 1 kJ/mol.

When the open–open isomer **2(o–o)** is irradiated with UV light for a few seconds on the substrate *in situ*, the remarkable change in ordering shown in Figure 5 was observed. Figure 5a shows the arrangement of **2(o–o)** before UV irradiation. After UV irradiation, there appeared a new arrangement that has a different line spacing of  $2.2 \pm 0.2$  nm as shown in Figure 5b.



**Figure 4.** (a) STM image of an arrangement of **2(o–o)** at the interface of octanoic acid–HOPG ( $100 \times 100$  nm<sup>2</sup>,  $I_{\text{set}} = 10$  pA,  $V_{\text{bias}} = -2.0$  V). (b) Small-area image of **2(o–o)** ( $25 \times 25$  nm<sup>2</sup>,  $I_{\text{set}} = 10$  pA,  $V_{\text{bias}} = -1.5$  V). (c) Structural model for **2(o–o)**. Orange line denotes the direction of the lines in the image.

This change is due to the photoisomerization of the diarylethene moiety. Furthermore, subsequent irradiation with visible light for about 10 min gave the original arrangement of **2(o–o)**.

As discussed with regard to **1**, surface exchange of adsorbed molecules with isomers in solution will occur after a photochromic reaction.<sup>10b</sup> After UV irradiation, three isomers should exist in the solution phase: the open–open, open–closed, and closed–closed isomers. In this system, not only the open–closed isomer but also the closed–closed isomer was easily formed because the two diarylethene moieties were separated from each other by a long distance. To investigate which isomer contributes to this new ordering, an STM measurement of the pure open–closed isomer **2(o–c)** and the closed–closed isomer **2(c–c)**, which were separated by the HPLC, was carried out.

Figure 6 shows the STM image of the open–closed isomer **2(o–c)**. The arrangement of **2(o–c)** also consists of parallel lines that are similar to those seen for **2(o–o)**. Each line consists of a lamellar structure (Figure 6b). The line spacing of **2(o–c)** was found to be 4.7 nm, which is slightly shorter than that of **2(o–o)**. The unit cell parameters are  $a = 2.2 \pm 0.2$  nm,  $b = 5.1 \pm 0.3$  nm, and  $\alpha = 86 \pm 3^\circ$ . The calculated structural model of **2(o–c)** is displayed in Figure 6c. Judging from this parameter set, the ordering of **2(o–c)** is not identical with either of the ordering of **2(o–o)** or the new ordering after UV irradiation. Although **2(o–c)** contains both open and closed isomers in one molecule, the two different isomers could not be distinguished in the image.

The ordering of the closed–closed isomer **2(c–c)** is completely different from that of **2(o–o)**. As shown in Figure 7, the ordering also consists of parallel lines. The line spacing of  $1.9 \pm 0.2$  nm is much narrower than that of **2(o–o)**, but very similar to the new ordering which appeared after UV irradiation. The new ordering in Figure 5 is assigned to the arrangement of **2(c–c)**. Figure 7b shows an expanded image. One bright ellipse spot and the other spot make the unit cell. The unit cell parameters are  $a = 2.6 \pm 0.2$  nm,  $b = 5.3 \pm 0.1$  nm, and  $\alpha = 40 \pm 3^\circ$ . Some of the brightest ellipses are only half the size

(18) (a) Hirose, T.; Matsuda, K.; Irie, M. *J. Org. Chem.* **2006**, *71*, 7499–7508. (b) Hamazaki, T.; Matsuda, K.; Kobatake, S.; Irie, M. *Bull. Chem. Soc. Jpn.* **2007**, *80*, 365–370.

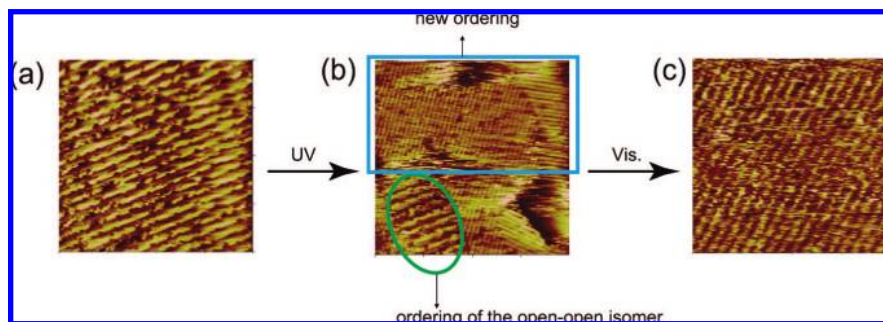


**Figure 5.** Sequence of STM images at the interface of octanoic acid–HOPG upon UV and visible irradiation of compound **2(o–o)** ( $100 \times 100 \text{ nm}^2$ , the same areas of the sample): (a) before UV irradiation,  $I_{\text{set}} = 10 \text{ pA}$ ,  $V_{\text{bias}} = -2.0 \text{ V}$ ; (b) after UV irradiation for 5 s ( $I_{\text{set}} = 10 \text{ pA}$ ,  $V_{\text{bias}} = -2.5 \text{ V}$ ); (c) after successive visible irradiation ( $I_{\text{set}} = 10 \text{ pA}$ ,  $V_{\text{bias}} = -2.5 \text{ V}$ ).

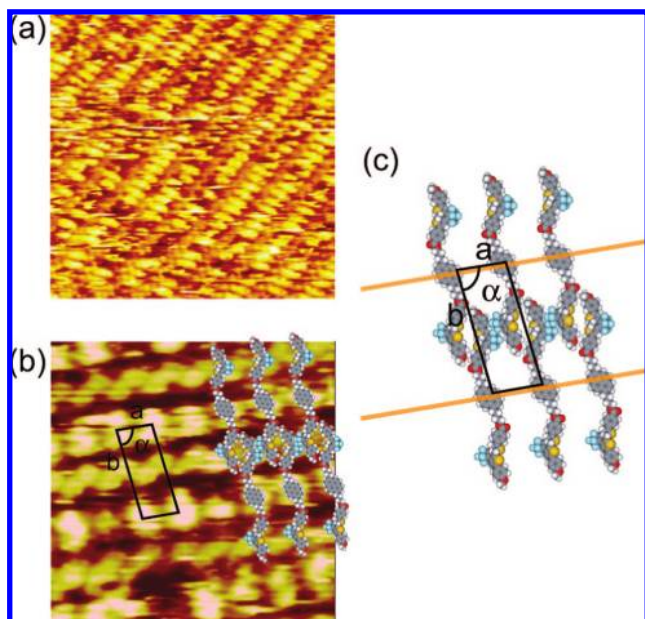


**Figure 6.** (a) STM image of an arrangement of **2(o–c)** at the interface of octanoic acid–HOPG ( $50 \times 50 \text{ nm}^2$ ,  $I_{\text{set}} = 10 \text{ pA}$ ,  $V_{\text{bias}} = -2.0 \text{ V}$ ). (b) Small-area image of **2(o–c)** ( $15 \times 15 \text{ nm}^2$ ,  $I_{\text{set}} = 10 \text{ pA}$ ,  $V_{\text{bias}} = -2.0 \text{ V}$ ). (c) Structural model for **2(o–c)**. Orange line denotes the direction of the lines in the image.

due to defects, suggesting that the brightest ellipse consists of two spots, namely, the densely packed two diarylethene moieties. The calculated structural model of **2(c–c)** is displayed in Figure 7c. The brightest ellipse represents two diarylethene moieties, the other spot represents the pyrene moiety, and the void between them represents the alkyl chains. In order to reproduce the observed arrangement, two diarylethene moieties need to be perpendicular to the HOPG surface. The closed-ring isomer of diarylethene has a flat structure, so that a dense packing is possible, as can also be seen in the above-mentioned closed isomer of the diarylethene monomer **1b**.

As discussed previously, the result of the molecular mechanics calculation indicates that the energy difference between the rotational isomers is very small. Therefore, the molecular conformation should depend on the environment. In the case of **2(c–c)**, the molecule is destabilized by adopting a perpendicular conformation between the pyrene ring and diarylethene, but the intermolecular stacking of the closed-form of diarylethenes compensates for this energy loss. The pyrene ring is parallel to the HOPG surface, which contributes the stabilization of the 2D structure.

Judging from these experiments, the new ordering in Figure 5 is assigned to the arrangement of **2(c–c)**. As mentioned

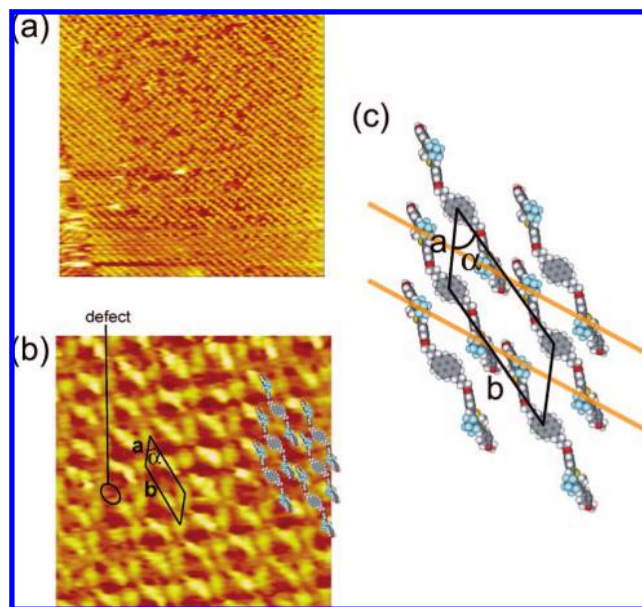


**Figure 7.** (a) STM image of an arrangement of **2(c–c)** at the interface of octanoic acid–HOPG ( $100 \times 100 \text{ nm}^2$ ,  $I_{\text{set}} = 10 \text{ pA}$ ,  $V_{\text{bias}} = -1.5 \text{ V}$ ). (b) Small-area image of **2(c–c)** ( $20 \times 20 \text{ nm}^2$ ,  $I_{\text{set}} = 10 \text{ pA}$ ,  $V_{\text{bias}} = -1.5 \text{ V}$ ). (c) Structural model for **2(c–c)**. Orange line denotes the direction of the lines in the image.

previously, the UV irradiation should give both the open–closed isomer **2(o–c)** and the closed–closed isomer **2(c–c)**, but the arrangement of **2(o–c)** was not observed. In order to examine the relative magnitudes of the adsorption process, we measured the STM image of the mixture with the ratio of o–o:o–c:c–c = 45:33:22 (Figure 8). The image predominantly consisted of the closed–closed isomer **2(c–c)** arrangement. This implies that **2(o–o)** and **2(o–c)** are less likely to be physisorbed on the HOPG surface than **2(c–c)**. This result also suggests that the domain of the **2(o–o)** existing in Figure 5b is a remnant of the initial **2(o–o)** arrangement domain.

For monomer **1**, the photoinduced ordering change was not observed, and only a disappearance of the ordering was observed. On the other hand, the ordering change was clearly observed for dimer **2**. This difference can be attributed to the higher stability of the 2D arrangement of the closed–closed isomer **2(c–c)** than that of the closed-ring isomer **1b**. The height of the pyrene moiety was around 0.17 nm in the image of **1a**, **2(o–o)**, **2(o–c)**, and **2(c–c)**, but in the image of **1b** the pyrene moiety was 0.43 nm high. This topographic data confirmed that the pyrene has perpendicular orientation to HOPG surface in **1b**, but is parallel in **1a**, **2(o–o)**, **2(o–c)**, and **2(c–c)**. The

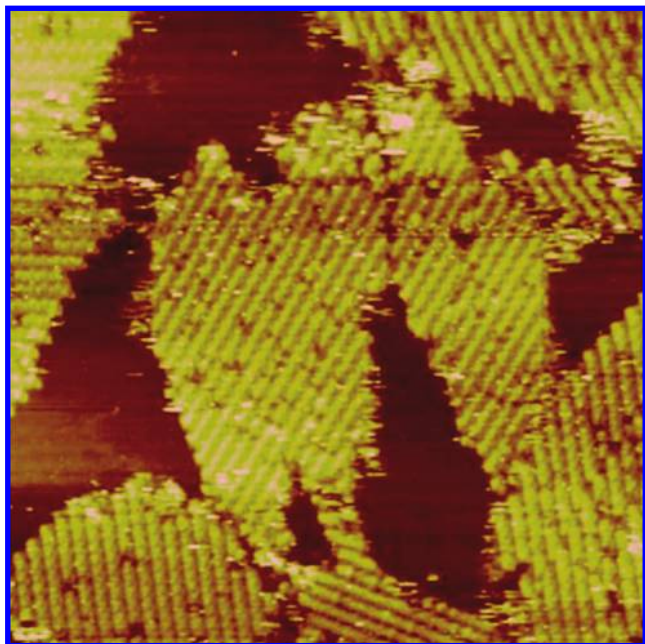


**Figure 8.** STM image of an arrangement of the mixture with the ratio of  $2(\mathbf{o}-\mathbf{o}):2(\mathbf{o}-\mathbf{c}):2(\mathbf{c}-\mathbf{c}) = 45:33:22$  at the interface of octanoic acid–HOPG ( $100 \times 100 \text{ nm}^2$ ,  $I_{\text{set}} = 10 \text{ pA}$ ,  $V_{\text{bias}} = -2.5 \text{ V}$ ).

**Table 1.** Unit Cell Parameters of Each Arrangement

isomer	a axis/nm	b axis/nm	angle/deg
$2(\mathbf{o}-\mathbf{o})$	$2.4 \pm 0.2$	$6.3 \pm 0.2$	$87 \pm 2$
$2(\mathbf{o}-\mathbf{c})$	$2.2 \pm 0.2$	$5.1 \pm 0.3$	$86 \pm 3$
$2(\mathbf{c}-\mathbf{c})$	$2.6 \pm 0.2$	$4.9 \pm 0.1$	$40 \pm 3$

difference in the stability of the 2D structure is attributed to this difference in the orientation of the pyrene ring.

Table 1 shows the unit cell parameters of all isomers. Each unit cell contains one molecule. By comparing the area of each unit cell, we can see that of  $2(\mathbf{c}-\mathbf{c})$  is the smallest; that is, the packing of the  $2(\mathbf{c}-\mathbf{c})$  is the densest of the three isomers. This is because the diarylethene moiety is lying perpendicular to the HOPG surface. In  $2(\mathbf{o}-\mathbf{o})$  and  $2(\mathbf{o}-\mathbf{c})$ , the *a* axes and the angles are almost identical; however, the *b* axis of  $2(\mathbf{o}-\mathbf{c})$  is shorter than that of  $2(\mathbf{o}-\mathbf{o})$ , suggesting that the packing of  $2(\mathbf{o}-\mathbf{c})$  is denser. There was no distinctive relationship between the orientation of the ordering of the adlayer and the orientation of the HOPG.

One of the advantages of using a diarylethene photochromic unit is the thermal stability of the photochromic isomers. In the previous study of De Schryver et al. using azobenzene,<sup>10b</sup> a photoinduced ordering change was reported, but a comparison with the ordering of the isolated isomers was not performed. In the present study, the separate arrangement of each of the isomers could be determined by isolating each isomer. In our system, the intermolecular interaction should be weaker than those in other systems having hydrogen bonding, metal–ligand interaction, or charge–transfer interaction. Here, the molecular assemblies have only a molecule–substrate interaction and van der Waals interaction between the alkyl chains; therefore, the 2D structure is not specially stabilized. However, this relatively weak adsorption energy on HOPG is preferable when studying an ordering change induced by external stimuli.

## Conclusions

We have studied the reversible photoinduced molecular ordering change of diarylethene derivatives having a pyrene

moiety at a solution–HOPG interface by STM. Different photochromic isomers showed different orderings, reflecting the differences in their molecular structures. For the diarylethene–pyrene–diarylethene triad, a new ordering appeared upon irradiation with UV light and returned to the original ordering upon irradiation with visible light. By comparison with the images of each isomer, the new arrangement was assigned to the ordering of the closed–closed isomer. The difference in the affinity to the substrate is thought to regulate the ordering behavior.

## Experimental Section

**Materials.** <sup>1</sup>H NMR spectra were recorded on a Bruker AVANCE 400 instrument. Mass spectra were obtained on a Shimadzu GC–MS–QP5050A and a JEOL JMS–GCmate II. All reactions were monitored by thin-layer chromatography carried out on 0.2-mm E. Merck silica gel plates (60F-254). Column chromatography was performed on silica gel (Kanto, 63–210 mesh).

**3-Bromo-2-methyl-5-(4-octyloxy-phenyl)thiophene (4).** To a solution of 2,4-dibromo-5-methylthiophene (**3**)<sup>19</sup> (8.0 g, 32 mmol) in dry THF (110 mL) was slowly added *n*-butyllithium hexane solution (1.6 M, 21 mL, 33 mmol) at  $-78 \text{ }^\circ\text{C}$  under an argon atmosphere. The solution was stirred for 30 min at  $-78 \text{ }^\circ\text{C}$ . After the addition of *tert*-butyl borate (13 mL, 33 mmol), the reaction mixture was further stirred for 1 h at  $-78 \text{ }^\circ\text{C}$ . The reaction was quenched by the addition of water. 1-Iodo-4-octyloxy-benzene<sup>20</sup> (10.0 g, 30 mmol), Pd(PPh<sub>3</sub>)<sub>4</sub> (500 mg, 0.43 mmol), and aqueous Na<sub>2</sub>CO<sub>3</sub> (20 wt %, 30 mL) were added to the solution. The solution was refluxed overnight. The reaction product was extracted with diethyl ether, and the organic layer was washed with brine, dried over MgSO<sub>4</sub>, filtered, and evaporated. The crude product was purified by silica gel column chromatography (chloroform) to yield **4** (6.5 g, 54%) as a white powder. <sup>1</sup>H NMR (CDCl<sub>3</sub>, TMS, 400 MHz)  $\delta$  0.89 (t, *J* = 7 Hz, 3 H), 1.28–1.43 (m, 10 H), 1.76 (quintet, *J* = 7 Hz, 2 H), 2.39 (s, 3 H), 3.96 (t, *J* = 7 Hz, 2 H), 6.68 (d, *J* = 9 Hz, 2 H), 6.89 (s, 1 H), 7.42 (d, *J* = 9 Hz, 2 H); FAB HRMS (*m/z*) [M]<sup>+</sup> Calcd for C<sub>19</sub>H<sub>25</sub>BrOS: 380.0809, Found: 380.0818.

**3-(2,3,3,4,4,5,5-Heptafluoro-cyclopent-1-enyl)-2-methyl-5-(4-octyloxy-phenyl)thiophene (5).** To a solution of compound **4** (3.0 g, 7.9 mmol) in dry THF (160 mL) was slowly added *n*-butyllithium hexane solution (1.6 M, 5.3 mL, 8.3 mmol) at  $-78 \text{ }^\circ\text{C}$  under an argon atmosphere. The solution was stirred for 1 h at  $-78 \text{ }^\circ\text{C}$ . After the addition of perfluorocyclopentene (3.4 mL, 24 mmol), the reaction mixture was further stirred for 1 h at that temperature. The reaction was quenched by the addition of water. The reaction product was extracted with diethyl ether and the organic layer was washed with brine, dried over MgSO<sub>4</sub>, filtered, and evaporated. The crude product was purified by silica gel column chromatography (hexane/dichloromethane = 9:1) to yield **5** (2.9 g, 74%) as a white powder. <sup>1</sup>H NMR (CDCl<sub>3</sub>, TMS, 400 MHz)  $\delta$  0.89 (t, *J* = 7 Hz, 3 H), 1.28–1.43 (m, 10 H), 1.76 (quintet, *J* = 7 Hz, 2 H), 2.39 (s, 3 H), 3.96 (t, *J* = 7 Hz, 2 H), 6.92 (d, *J* = 9 Hz, 2 H), 7.13 (s, 1 H) 7.45 (d, *J* = 9 Hz, 2 H); FAB HRMS (*m/z*) [M]<sup>+</sup> Calcd for C<sub>24</sub>H<sub>25</sub>F<sub>7</sub>OS: 494.1514, Found: 494.1517.

**2-[4-(4-{3,3,4,4,5,5-Hexafluoro-2-[2-methyl-5-(4-octyloxy-phenyl)-thiophen-3-yl]-cyclopent-1-enyl}-5-methyl-thiophen-2-yl)-phenyl]-[1,3]dioxolane (6).** To a solution of compound **5** (0.90 g, 2.8 mmol) in dry THF (50 mL) was slowly added *n*-butyllithium hexane solution (1.6 M, 1.9 mL, 3.1 mmol) at  $-78 \text{ }^\circ\text{C}$  under an argon atmosphere. The solution was stirred for 1 h at  $-78 \text{ }^\circ\text{C}$ . After the addition of 3-bromo-5-(4-(2,5-dioxolanyl)-phenyl)-2-methylthiophene<sup>21</sup> (1.5 g, 3.0 mmol) in dry THF (30 mL), the reaction mixture was further stirred for 1 h at that temperature.

(19) Reinecke, M. G.; Adickers, H. W.; Pyun, C. *J. Org. Chem.* **1971**, *36*, 2690–2692.

(20) Chang, J. Y.; Baik, J. H.; Lee, C. B.; Han, M. J.; Hong, S.-K. *J. Am. Chem. Soc.* **1997**, *119*, 3197–3198.



The reaction was quenched by the addition of water. The reaction product was extracted with diethyl ether, and the organic layer was washed with brine, dried over  $\text{MgSO}_4$ , filtered, and evaporated. The crude product was purified by silica gel column chromatography (dichloromethane) to yield **6** (1.20 g, 61%) as a yellow powder.  $^1\text{H}$  NMR ( $\text{CDCl}_3$ , TMS, 400 MHz)  $\delta$  0.89 (t,  $J = 7$  Hz, 3 H), 1.25–1.50 (m, 10 H), 1.79 (quintet,  $J = 7$  Hz, 2 H), 1.93 (s, 3 H), 1.97 (s, 3 H), 3.75 (t,  $J = 7$  Hz, 2 H), 4.05–4.15 (m, 4 H), 5.85 (s, 1 H), 6.90 (d,  $J = 9$  Hz, 2 H), 7.14 (s, 1H), 7.29 (s, 1 H), 7.44 (d,  $J = 9$  Hz, 2 H), 7.49 (d,  $J = 8$  Hz, 2 H), 7.55 (d,  $J = 8$  Hz, 2 H); FAB HRMS ( $m/z$ ) [ $\text{M}]^+$  Calcd for  $\text{C}_{38}\text{H}_{38}\text{F}_6\text{O}_3\text{S}_2$ : 720.2167, Found: 720.2160.

**4-(4-{3,3,4,4,5,5-Hexafluoro-2-[2-methyl-5-(4-octyloxy-phenyl)-thiophen-3-yl]-cyclopent-1-enyl}-5-methyl-thiophen-2-yl)-benzaldehyde (7).** To a solution of compound **6** (600 mg, 0.83 mmol) in wet acetone (50 mL) was added pyridinium *p*-toluenesulfonate (500 mg, 2.00 mmol) at room temperature. The solution was refluxed overnight. After cooling, the reaction mixture was poured into water and extracted with diethyl ether, and the organic layer was washed with brine, dried over  $\text{MgSO}_4$ , filtered, and evaporated. The crude product was purified by silica gel column chromatography (hexane/dichloromethane = 4:6) to yield **7** (450 mg, 77%) as a yellow amorphous.  $^1\text{H}$  NMR ( $\text{CDCl}_3$ , TMS, 400 MHz)  $\delta$  0.89 (t,  $J = 7$  Hz, 3 H), 1.28–1.43 (m, 10 H), 1.76 (quintet,  $J = 7$  Hz, 2 H), 2.39 (s, 3 H), 3.96 (t,  $J = 7$  Hz, 2 H), 6.85 (d,  $J = 9$  Hz, 2 H), 7.14 (s, 1 H), 7.29 (s, 1 H), 7.43 (d,  $J = 9$  Hz, 2 H), 7.46 (d,  $J = 8$  Hz, 2 H), 7.54 (d,  $J = 8$  Hz, 2 H); FAB HRMS ( $m/z$ ) [ $\text{M}]^+$  Calcd for  $\text{C}_{36}\text{H}_{34}\text{F}_6\text{O}_2\text{S}_2$ : 676.1904, Found: 676.1907.

**4-(4-{3,3,4,4,5,5-Hexafluoro-2-[2-methyl-5-(4-octyloxy-phenyl)-thiophen-3-yl]-cyclopent-1-enyl}-5-methyl-thiophen-2-yl)benzoic Acid (8).** Jones reagent, which was prepared from  $\text{CrO}_3$  (43 mg, 0.43 mmol),  $\text{H}_2\text{SO}_4$  (0.03 mL), and  $\text{H}_2\text{O}$  (1 mL) was added dropwise to a stirred solution of **7** (450 mg, 0.66 mmol) in acetone (70 mL) at room temperature and further stirred for overnight. The reaction mixture was extracted with diethyl ether and the organic layer was washed with brine, dried over  $\text{MgSO}_4$ , filtered, and evaporated. The crude product was purified by silica gel column chromatography (dichloromethane) to yield **8** (450 mg, 77.0%) as a green powder.  $^1\text{H}$  NMR ( $\text{CDCl}_3$ , TMS, 400 MHz)  $\delta$  0.90 (t,  $J = 6$  Hz, 3 H), 1.28–1.43 (m, 10 H), 1.79 (quintet,  $J = 8$  Hz, 2 H), 1.95 (s, 3 H), 1.99 (s, 3 H), 3.97 (t,  $J = 6$  Hz, 2 H), 6.90 (d,  $J = 9$  Hz, 2 H), 7.15 (s, 1 H), 7.41 (s, 1 H), 7.44 (d,  $J = 9$  Hz, 2 H), 7.63 (d,  $J = 8$  Hz, 2 H), 8.09 (d,  $J = 8$  Hz, 2 H); FAB HRMS ( $m/z$ ) [ $\text{M}]^+$  Calcd for  $\text{C}_{36}\text{H}_{34}\text{F}_6\text{O}_3\text{S}_2$ : 692.1854, Found: 692.1844.

**4-(4-{3,3,4,4,5,5-Hexafluoro-2-[2-methyl-5-(4-octyloxy-phenyl)-thiophen-3-yl]-cyclopent-1-enyl}-5-methyl-thiophen-2-yl)benzoic Acid 4-Pyren-1-yl-butyl Ester (1a).** To a solution of **8** (250 mg, 0.35 mmol) in dry DMF (4 mL), DCC (141 mg, 0.46 mmol), DMAP (55 mg, 0.46 mmol) and 1-pyrenebutanol (130 mg, 0.46 mmol) was added at room temperature. The solution was stirred for 7 h. The reaction was quenched by the addition of 2-propanol. The reaction product was extracted with ethyl acetate, and the organic layer was washed with brine, dried over  $\text{MgSO}_4$ , filtered, and evaporated. The crude product was purified by silica gel column chromatography (dichloromethane) to yield **1** (80 mg, 24%) as a yellow powder.  $^1\text{H}$  NMR ( $\text{CDCl}_3$ , TMS, 400 MHz)  $\delta$  0.90 (t,  $J = 5.6$  Hz, 3 H), 1.28–1.43 (m, 10 H), 1.79 (quintet,  $J = 8$  Hz, 2 H), 1.94–2.06 (m, 10 H), 3.44 (t,  $J = 7$  Hz, 2 H), 3.97 (t,  $J = 6$  Hz, 2 H), 4.40 (t,  $J = 6$  Hz, 2 H), 6.89 (d,  $J = 9$  Hz, 2 H), 7.15 (s, 1 H), 7.36 (s, 1 H), 7.44 (d,  $J = 9$  Hz, 2 H), 7.52 (d,  $J = 8$  Hz, 2 H), 7.89 (d,  $J = 8$  Hz, 1 H), 7.94 (d,  $J = 8$  Hz, 2 H), 7.99–8.17 (m, 7 H), 8.28 (d,  $J = 9$  Hz, 2 H); UV–vis (AcOEt)  $\lambda_{\text{max}}$  ( $\epsilon$ ) 276 ( $7.1 \times 10^4$ ) nm; FAB HRMS ( $m/z$ ) [ $\text{M}]^+$  Calcd for  $\text{C}_{56}\text{H}_{50}\text{F}_6\text{O}_3\text{S}_2$ : 948.3106, Found: 948.3129.

Corresponding closed-ring isomer **1b**. After irradiation with UV light, the mixture was separated by HPLC (column: Wakosil 5SIL

(10–250 mm), eluent: hexane/AcOEt = 95:5, flow: 3 mL/min, retention time: **1a** = 30 min; **1b** = 26 min). UV–vis (AcOEt)  $\lambda_{\text{max}}$  ( $\epsilon$ ) 606 ( $2.0 \times 10^4$ ) nm.

**2-[4-(4-{3,3,4,4,5,5-Hexafluoro-2-[5-(4-methoxymethoxy-phenyl)-2-methyl-thiophen-3-yl]-cyclopent-1-enyl}-5-methyl-thiophen-2-yl)-phenyl]-[1,3]dioxolane (11).** To a solution of 2,4-dibromo-5-methylthiophene (**3**)<sup>19</sup> (2.9 g, 11.4 mmol) in dry THF (40 mL) was slowly added *n*-butyllithium hexane solution (1.6 M, 9.7 mL, 15.5 mmol) at  $-78$  °C under an argon atmosphere. The solution was stirred for 30 min at  $-78$  °C. After the addition of *tert*-butyl borate (6 mL, 15.6 mmol), the reaction mixture was further stirred for 1 h at  $-78$  °C. The reaction was quenched by the addition of water. 1-Bromo-4-methoxymethoxy-benzene (3.0 g, 11.4 mmol),  $\text{Pd}(\text{PPh}_3)_4$  (200 mg, 0.17 mmol), and aqueous  $\text{Na}_2\text{CO}_3$  (20 wt %, 30 mL) were added to the solution. The solution was refluxed overnight. The reaction product was extracted with diethyl ether, and the organic layer was washed with brine, dried over  $\text{MgSO}_4$ , filtered, and evaporated. The crude product was purified by silica gel column chromatography (chloroform:hexane = 1:2) to yield bromothiophene derivative **9** (2.8 g, 79%) as a white powder.  $^1\text{H}$  NMR ( $\text{CDCl}_3$ , TMS, 400 MHz)  $\delta$  2.40 (s, 3 H), 3.48 (s, 3 H), 5.19 (s, 2 H), 6.99 (s, 1 H), 70.04 (d,  $J = 9$  Hz, 2 H), 7.42 (d,  $J = 9$  Hz, 2 H); EI MS ( $m/z$ ) [ $\text{M}]^+$  312, 314.

To a solution of compound **9** (5.0 g, 16 mmol) in dry THF (250 mL) was slowly added *n*-butyllithium hexane solution (1.6 M, 11.2 mL, 1.8 mmol) at  $-78$  °C under an argon atmosphere. The solution was stirred for 1 h at  $-78$  °C. After the addition of perfluorocyclopentene (8.0 mL, 56 mmol), the reaction mixture was further stirred for 1 h at  $-78$  °C. The reaction was quenched by the addition of water. The reaction product was extracted with diethyl ether, and the organic layer was washed with brine, dried over  $\text{MgSO}_4$ , filtered, and evaporated. The crude product was purified by silica gel column chromatography (hexane/dichloromethane = 1:1) to yield compound **10** (5.3 g, 77%) as a white powder.  $^1\text{H}$  NMR ( $\text{CDCl}_3$ , TMS, 400 MHz)  $\delta$  2.46 (d,  $J = 3$  Hz, 3 H), 3.49 (s, 3 H), 5.19 (s, 2H), 7.00 (s, 1 H), 7.03 (d,  $J = 9$  Hz, 2 H) 7.42 (d,  $J = 9$  Hz, 2 H); EI MS ( $m/z$ ) [ $\text{M}]^+$  426.

To a solution of 3-bromo-5-(4-(2,5-dioxolanyl)phenyl)-2-methylthiophene (1.3 g, 3.95 mmol) in dry THF (80 mL) was slowly added *n*-butyllithium hexane solution (1.6 M, 2.7 mL, 4.3 mmol) at  $-78$  °C under an argon atmosphere. The solution was stirred for 1 h at  $-78$  °C. After the addition of compound **10** (2.1 g, 5.0 mmol) in dry THF (30 mL), the reaction mixture was further stirred for 1 h at  $-78$  °C. The reaction was quenched by the addition of water. The reaction product was extracted with diethyl ether, and the organic layer was washed with brine, dried over  $\text{MgSO}_4$ , filtered, and evaporated. The crude product was purified by silica gel column chromatography (dichloromethane) to yield compound **11** (2.3 g, 89%) as a light green powder.  $^1\text{H}$  NMR ( $\text{CDCl}_3$ , TMS, 400 MHz)  $\delta$  1.94 (s, 3 H), 1.97 (s, 3 H), 3.48 (s, 3 H), 4.05–4.15 (m, 4 H), 5.20 (s, 2 H), 5.83 (s, 1 H), 7.05 (d,  $J = 9$  Hz, 2 H), 7.16 (s, 1 H), 7.28 (s, 1 H), 7.45 (d,  $J = 9$  Hz, 2 H), 7.49 (d,  $J = 8$  Hz, 2 H), 7.55 (d,  $J = 8$  Hz, 2 H); FAB HRMS ( $m/z$ ) [ $\text{M}]^+$  Calcd for  $\text{C}_{32}\text{H}_{26}\text{F}_6\text{O}_4\text{S}_2$ : 652.1177, Found: 652.1190.

**4-(4-{2-[5-(4-Dodecyloxy-phenyl)-2-methyl-thiophen-3-yl]-3,3,4,4,5,5-hexafluoro-cyclopent-1-enyl}-5-methyl-thiophen-2-yl)benzaldehyde (13).** To a solution of compound **11** (0.5 g, 0.77 mmol) in dry THF (40 mL) was slowly added HCl aq. (35%, 5 mL) at room temperature. The solution was stirred overnight at room temperature. The reaction product was extracted with diethyl ether, and the organic layer was washed with brine, dried over  $\text{MgSO}_4$ , filtered, and evaporated to give compound **12**. The crude product was not further purified and used in the next reaction.

To a solution of compound **12** (0.5 g, 0.88 mmol) in ethanol (10 mL) was added KOH (50 mg, 0.89 mmol), KI (1 mg, cat.) and 1-bromododecane (2 g, 8.9 mmol) at room temperature. The solution was refluxed overnight. The reaction product was extracted with diethyl ether, and the organic layer was washed with brine, dried over  $\text{MgSO}_4$ , filtered, and evaporated. The crude product was

(21) Yamamoto, S.; Matsuda, K.; Irie, M. *Chem. Eur. J.* **2003**, *9*, 4878–4886.

purified by silica gel column chromatography (hexane/dichloromethane = 1:1) to yield **13** (540 mg, 96%) as a green powder.  $^1\text{H NMR}$  ( $\text{CDCl}_3$ , TMS, 400 MHz)  $\delta$  0.88 (t,  $J = 7$  Hz, 3 H), 1.27–1.45 (m, 18 H), 1.79 (quint,  $J = 8$  Hz, 2 H), 1.95 (s, 3 H), 2.00 (s, 3 H), 3.97 (t,  $J = 7$  Hz, 2 H), 6.90 (d,  $J = 9$  Hz, 2 H), 7.15 (s, 1 H), 7.43 (s, 1 H), 7.44 (d,  $J = 9$  Hz, 2 H), 7.69 (d,  $J = 8$  Hz, 2 H), 7.89 (d,  $J = 8$  Hz, 2 H), 10.00 (s, 1 H); FAB HRMS ( $m/z$ ) [ $M$ ] $^+$  Calcd for  $\text{C}_{40}\text{H}_{42}\text{F}_6\text{O}_2\text{S}_2$ : 732.2530, Found: 732.2518.

**4-(4-{2-[5-(4-Dodecyloxy-phenyl)-2-methyl-thiophen-3-yl]-3,3,4,4,5,5-hexafluoro-cyclopent-1-enyl}-5-methyl-thiophen-2-yl)benzoic Acid (14).** Jones reagent, which was prepared from  $\text{CrO}_3$  (43 mg, 0.43 mmol),  $\text{H}_2\text{SO}_4$  (0.03 mL), and  $\text{H}_2\text{O}$  (1 mL) was added dropwise to a stirred solution of **13** (540 mg, 0.74 mmol) in acetone (50 mL) at room temperature and further stirred overnight. The reaction mixture was extracted with diethyl ether, and the organic layer was washed with brine, dried over  $\text{MgSO}_4$ , filtered, and evaporated. The crude product was purified by silica gel column chromatography (dichloromethane) to yield **14** (450 mg, 77.0%) as a green powder.  $^1\text{H NMR}$  ( $\text{CDCl}_3$ , TMS, 400 MHz)  $\delta$  0.88 (t,  $J = 7$  Hz, 3 H), 1.27–1.45 (m, 18 H), 1.79 (quint,  $J = 8$  Hz, 2 H), 1.95 (s, 3 H), 2.00 (s, 3 H), 3.97 (t,  $J = 7$  Hz, 2 H), 6.90 (d,  $J = 9$  Hz, 2 H), 7.15 (s, 1 H), 7.42 (s, 1 H), 7.44 (d,  $J = 9$  Hz, 2 H), 7.63 (d,  $J = 8$  Hz, 2 H), 8.11 (d,  $J = 8$  Hz, 2 H); FAB HRMS ( $m/z$ ) [ $M$ ] $^+$  Calcd for  $\text{C}_{40}\text{H}_{42}\text{F}_6\text{O}_3\text{S}_2$ : 748.2480, Found: 748.2483.

**4-[6-(4-Hydroxy-but-1-ynyl)-pyren-1-yl]-but-3-yn-1-ol (17).** To a solution of pyrene **15** (5 g, 24.7 mmol) in  $\text{CH}_2\text{Cl}_2/\text{MeOH}$  (= 5:2, 100 mL) was added benzyltrimethylammonium tribromide (19.3 g, 49.4 mmol) and  $\text{ZnCl}_2$  (0.5 g, cat.), and the solution was stirred overnight at room temperature. The precipitation formed was filtered using Büchner funnel, washed with hexane, dried *in vacuo* to give 1,6-dibromopyrene **16** (8.6 g, quant.) as a mixture of 1,6-isomer **16** and 1,8-isomer **16'**. The crude product was not further purified.

To a solution of **16** (2.0 g, 5.6 mmol) in morpholine (69 mL) was added 3-butyn-1-ol (2.5 g, 34 mmol),  $\text{Pd}(\text{Ph}_3\text{P})_2\text{Cl}_2$  (100 mg, cat.) and  $\text{CuI}$  (14 mg, cat.). The solution was deoxygenated by argon bubbling and stirred overnight at 100 °C. After cooling the reaction mixture, the yellow precipitation was filtered and washed with hexane. Separation of 1,8-isomer **17'** was performed by silica gel column chromatography (AcOEt) to yield compound **17** (90 mg, 4.6%) as a yellow powder.  $^1\text{H NMR}$  ( $\text{CDCl}_3$ , TMS, 400 MHz)  $\delta$  2.95 (t,  $J = 6$  Hz, 4 H), 3.99 (t,  $J = 6$  Hz, 4 H), 8.09–8.12 (m, 6 H), 8.55 (d,  $J = 9$  Hz, 2 H); FAB HRMS ( $m/z$ ) [ $M$ ] $^+$  Calcd for  $\text{C}_{24}\text{H}_{18}\text{O}_2$ : 338.1307, Found: 338.1318.

**4-[6-(4-Hydroxy-butyl)-pyren-1-yl]-butan-1-ol (18).** To a solution of **17** (90 mg, 0.27 mmol) in AcOEt (10 mL) was added 5% Pd–C (100 mg), and the mixture was stirred under a  $\text{H}_2$  atmosphere (1 atm) for overnight. The catalyst was removed by using a Celite column to yield **18** (90 mg, quant.) as a light yellow powder.  $^1\text{H NMR}$  ( $\text{CDCl}_3$ , TMS, 400 MHz)  $\delta$  1.75 (quint.,  $J = 7$  Hz, 4 H), 1.93 (quint.,  $J = 8$  Hz, 4 H), 3.38 (t,  $J = 6$  Hz, 4 H), 3.70 (t,  $J = 6$  Hz, 4 H), 7.85 (d,  $J = 8$  Hz, 2 H), 8.05 (d,  $J = 9$  Hz, 2 H), 8.09 (d,  $J = 8$  Hz, 2 H), 8.22 (d,  $J = 9$  Hz, 2 H); FAB HRMS ( $m/z$ ) [ $M$ ] $^+$  Calcd for  $\text{C}_{24}\text{H}_{26}\text{O}_2$ : 346.1933, Found: 346.1937.

**1,6-bis-[4-(4-{2-[5-(4-Dodecyloxy-phenyl)-2-methyl-thiophen-3-yl]-3,3,4,4,5,5-hexafluoro-cyclopent-1-enyl}-5-methyl-thiophen-2-yl)]-benzoic acid (Pyrene-1,6-diyl)bis(butane-1,4-diyl) Ester (2(o–o)).** To a solution of **14** (230 mg, 0.31 mmol) in dry  $\text{CH}_2\text{Cl}_2$  (10 mL), DCC (110 mg, 0.36 mmol), DMAP (44 mg, 0.36 mmol) and **18** (50 mg, 0.15 mmol) was added at room temperature. The solution was stirred for 7 h. The reaction was quenched by the addition of 2-propanol. The reaction product was extracted with ethyl acetate, and the organic layer was washed with brine, dried over  $\text{MgSO}_4$ , filtered, and evaporated. The crude product was purified by silica gel column chromatography (chloroform) to yield **2** (120 mg, 45%) as a white powder.  $^1\text{H NMR}$  ( $\text{CDCl}_3$ , TMS, 400 MHz)  $\delta$  0.80 (t,  $J = 7$  Hz, 6 H), 1.28–1.44 (m, 36 H), 1.79 (quint.,  $J = 8$  Hz, 4 H), 1.94–2.05 (m, 20 H), 3.43 (t,  $J = 7$  Hz, 4 H),

3.97 (t,  $J = 6$  Hz, 4 H), 4.40 (t,  $J = 6$  Hz, 4 H), 6.89 (d,  $J = 8$  Hz, 4 H), 7.14 (s, 2H), 7.36 (s, 2 H), 7.43 (d,  $J = 8$  Hz, 4 H), 7.53 (d,  $J = 8$  Hz, 4 H), 7.87 (d,  $J = 8$  Hz, 2 H), 7.99 (d,  $J = 8$  Hz, 4 H), 8.04 (d,  $J = 9$  Hz, 2 H), 8.10 (d,  $J = 8$  Hz, 2 H), 8.22 (d,  $J = 9$  Hz, 2 H); UV–vis (AcOEt)  $\lambda_{\text{max}}$  ( $\epsilon$ ) 279 ( $1.0 \times 10^5$ ) nm; MALDI-TOF MS [ $M$ ] $^+$  1806.225.

**Corresponding Closed–Closed Isomer 2(c–c).** After irradiation with UV light, the mixture was separated by HPLC (column: Wakosil 5SIL (10–250 mm), eluent: hexane/ $\text{CH}_2\text{Cl}_2 = 35:65$ , flow: 5 mL/min, retention time: **2(o–o)** = 17 min; **2(o–c)** = 14 min; **2(c–c)** = 12 min). UV–vis (AcOEt)  $\lambda_{\text{max}}$  ( $\epsilon$ ) 605 ( $4.2 \times 10^4$ ) nm.

**STM Measurement.** All STM experiments were performed at room temperature and ambient conditions. The STM images were acquired with a Digital Instruments Multimode Nanoscope IIIa and IV and obtained at the liquid–solid interface. The measurement was performed in the low-current mode. All STM images were acquired in constant current mode. The STM tips were mechanically cut from Pt/Ir (80%/20%). Highly oriented pyrolytic graphite purchased from the Veeco Metrology Group was used as a substrate. An almost saturated solution ( $\sim 10^{-3}$  M) of compound **1** in 1-phenyloctane and compound **2** in octanoic acid ( $\sim 10^{-5}$  M) was used. The image of compound **2** could not be obtained at the 1-phenyloctane–HOPG interface, so that the compound was observed at the octanoic acid–HOPG interface. These solvents were purchased from Aldrich and used without further purification. A drop of the solution was deposited onto freshly cleaved HOPG, and the tip was immersed into the solution and the image scanned. Photoirradiation study for STM investigation was performed using a Moritex 200 W mercury–xenon lamp equipped with an optical fiber. UV light ( $11 \text{ mW/cm}^2$ ,  $300 \text{ nm} < \lambda < 390 \text{ nm}$ ) and visible light ( $480 \text{ nm} < \lambda$ ) were used for the photoreaction. All STM images contain raw data and were not subjected to any manipulation or imaging processing. Images were analyzed by using the graphite substrate as a calibration grid.

**Photochemical Measurement.** Absorption spectra were measured on a Hitachi U-3500 spectrophotometer. Photoirradiation was carried out with a USHIO 500 W superhigh pressure mercury lamp with a combination of an optical filter and a monochromator (Ritsu MC-10N).

**X-ray Crystallographic Analysis.** X-ray crystallographic analysis of **1a** was performed using a Bruker SMART 1000 CCD-based diffractometer (55 kV, 35 mA) with Mo  $K\alpha$  radiation. The structure was solved by direct methods and refined by full least-squares on  $F^2$  using the SHELXTL software package. The positions of all hydrogen atoms were calculated geometrically and refined by the riding model. CCDC 650023 contains the supplementary crystallographic data.

**Molecular Modeling.** Molecular modeling in gas phase was performed by force field structure optimization using MacroModel 9.1 (OPLS\_2005 forcefield). Conformational sampling was carried out by the Monte Carlo torsional sampling. For the molecules **2(o–o)**, **2(o–c)**, and **2(c–c)**, the calculation was performed without alkyl chains. The calculated structures and the Cartesian coordinates are shown in Supporting Information.

**Acknowledgment.** This work was partially supported by PRESTO, JST and a Grant-in-Aid for Science Research in a Priority Area “New Frontiers in Photochromism” (471) (No. 19050009) from the Ministry of Education, Culture, Sports, Science and Technology (MEXT), Japan.

**Supporting Information Available:** Results of the molecular mechanics calculation, and the optimized Cartesian coordinates; crystallographic data of compound **1a** in CIF format. This material is available free of charge via the Internet at <http://pubs.acs.org>.

JA711041P